Diagn Interv Radiol 2013; 19:418-426

INTERVENTIONAL RADIOLOGY
ORIGINAL ARTICLE

Three-dimensional rotational angiography is preferable to conventional two-dimensional techniques for uterine artery embolization

Atul Gupta, Kirsten Zuurmond, Thijs Grünhagen, Geert Maleux

PURPOSE
We aimed to investigate the potential benefits of three-dimensional rotational angiography (3DRA) compared to two-dimensional (2D) roadmapping to visualize the uterine artery (UA) origins during uterine artery embolization (UAE) procedures.

MATERIALS AND METHODS
Sixty-three UAE cases performed under 3DRA guidance were reviewed retrospectively to determine if there was an optimal angiographic projection angle for identifying UA origin. Digital subtraction angiogram (DAS)-like images of the pelvic vessels were generated from the 3DRA scans at six different angles: left anterior oblique (LAO) 25°, 35°, 45°; and right anterior oblique (RAO) 25°, 35°, 45°. Two experienced interventional radiologists assessed if these angles could effectively serve as a roadmap to guide catheterization of the UA. Assessment was validated against original 3DRA scans to determine the percentage of true and false positives.

RESULTS
No single projection angle was found that could consistently be utilized for UA catheterization. The projection angles used during 3D roadmapping for both the left and right UA showed two clusters with both a wide spread: RAO 20° to 50° and LAO 20° to 50°. More than 50% of the DSA-like images at RAO and LAO 45° appeared to be adequate for UA catheterization, but validation against the 3DRA revealed 28% of these images were suboptimal and deceptive, due to unappreciated overlapping vessels.

CONCLUSION
No standard projection angles can be recommended with 2D roadmapping to consistently visualize UA origin. The 3DRA can be as a useful tool for UAE to achieve reliable and consistent visibility of the UA origin.

From the Department of Interventional Radiology (A.G. ✉ *guptaa@mlhs.org*), Paoli Hospital, Paoli, Pennsylvania, USA; Philips Healthcare (K.Z., T.G.), Best, The Netherlands; the Department of Radiology (G.M.), University Hospital Gasthuisberg, Leuven, Belgium.

Received 8 November 2012; revision requested 26 December 2012; revision received 11 January 2013; accepted 29 January 2013.

Published online 10 April 2013.
DOI 10.5152/dir.2013.130

Uterine artery embolization (UAE) has shown to be a valuable, minimally invasive alternative for the treatment of women with symptomatic leiomyomas, uterine vascular malformations, and postpartum hemorrhage (1–9). The procedure is performed with angiographic and fluoroscopic guidance. One disadvantage of this treatment is the exposure of the uterus and ovaries to radiation. A considerable number of patients are women of childbearing age, making it especially important to keep the dose as low as reasonably achievable. Several methods have been suggested to reduce the dose, including bilateral femoral access and low imaging frame rates (10–12). Additionally, it has been shown that the interventionist's experience has a strong impact on reducing the number of runs needed to determine the best uterine artery (UA) catheterization angle, and therefore reducing the total radiation dose (13).

The current and established technique of UA catheterization relies on the physician choosing a somewhat arbitrary starting projection or angle, with a subsequent pelvic digital subtraction angiogram (DSA). This initially chosen projection is often suboptimal, and one or even several additional X-ray acquisitions are performed before the UA can be catheterized. DSA acquisitions are a major contributor to the total radiation administered to the patient (13). Therefore, minimizing the number of DSA runs has been associated with a lower patient dose and a reduction of the amount of administered iodinated contrast medium (14).

Three-dimensional rotational angiography (3DRA) has been introduced to overcome limitations of two-dimensional (2D) imaging, such as vessel foreshortening and vessel obscuration due to overlying vessels or bone. Three-dimensional (3D) volumes such as 3DRA and magnetic resonance (MR) angiography can show most branches of the internal iliac artery in addition to their point of origin (14–16). Therefore, 3DRA can be used as a mapping tool of the pelvic arterial tree for UAE.

Thus far, studies that used 3DRA scans (17) and MR angiography scans (15, 18) to determine the best position of the C-arm for catheterization of the UA revealed no single angulation that could be recommended for standard angiography. A limitation of the prior study using 3DRA scans was the low number of patients studied (n=8). Nevertheless, these studies show a wide spread when examining the preference in angiographic projection angles using 3D volumes. However, for each case, there might be multiple projection angles that could provide a good roadmap. Therefore, it may be important to analyze multiple projections from each 3DRA scan to assess whether one of these angles would suffice for most cases. Several factors might influence the angulation and rotation of the C-arm for the best view of the origin of the UA, such

as the anatomy of branching patterns of the internal iliac artery. Knowledge of the potential anatomical variants is important for those performing UAE.

The purpose of this study was to evaluate the use of 3DRA compared to 2D angiographic projection angles in correctly visualizing the origin of the UA for subsequent UAE, in the largest analysis to date.

Materials and methods

Patients

We retrospectively gathered the data from 63 patients treated with UAE using 3D roadmapping. Ethical committee approval was given for both centers participating in this trial (Paoli Hospital, Paoli, Pennsylvania, USA and University Hospital Gasthuisberg, Leuven, Belgium). Indicators for UAE were postpartum hemorrhage (n=2), placenta percreta (n=1), ectopic pregnancy (n=1), and vascular malformation (n=2). The remaining patients were treated for uterine leiomyomas (n=57).

Acquisition of 3D scans

All procedures were carried out on a Philips Allura Xper FD20 system (Philips Healthcare, Best, The Netherlands). The 3DRA was performed as part of routine clinical practice at both institutions. During the rotational acquisition, nonionic iodinated contrast material (Center 1: Optiray™ 320 [Ioversol Injection 68%, Mallinckrodt Inc., Hazelwood, Missouri, USA], Center 2: Iopromide [Ultravist 240, Bayer Schering Pharma, Brussels, Belgium]) was injected through a catheter placed into the vascular territory of interest. In Center 1 (30 patients), an aorta injection was performed and a total of 120 frames were acquired during a 240° rotation with the C-arm in the propeller position. In Center 2, (33 patients), a selective injection of both internal iliac arteries was used, and a total of 120 frames were obtained over a 180° rotation with the C-arm in the roll position. The images were automatically sent to a dedicated workstation, and a 3D volume was reconstructed within seconds of the acquisition.

Definition of working projections

Following assessment of the reconstructed 3D volume, suitable working projections for catheterization of the UAs were selected and stored in the workstation. The working projections are expressed as degrees of angulation (caudal-cranial movement of the C-arm) and rotation (left anterior oblique [LAO] and right anterior oblique [RAO] view). During the intervention, the stored working projections were recalled, and the C-arm was automatically steered to the corresponding angles. The 3DRA volume was then overlaid on live fluoroscopy to serve as a 3D-roadmap for catheterization of the UA.

We then retrospectively examined the stored working projections of our patient cohort to investigate if there were similar projection angles that were routinely used to view the origin of the UA. The image quality of the 3DRA results was graded by the interventional radiologists to examine whether these were sufficient to visualize the origin of the UA for subsequent roadmapping. A grading scale of 1–4 (poor, fair, good, and excellent, respectively) was used to define the image quality.

Comparison to DSA-like images

Following grading, DSA-like images (using maximum intensity projection [MIP]) were generated from the 3DRA scans at RAO 25°, 35°, and 45°; and LAO 25°, 35°, and 45° with the cranial-caudal angulation set at zero. These six projections were chosen since they are the typical projections used in routine clinical practice for 2D roadmapping. Two interventional radiologists, one from Center 1 (A.G.) and one from Center 2 (G.M.) (10 and 16 years of experience, respectively) blindly assessed the image quality of the total set of DSA-like images and evaluated whether they could effectively serve as a roadmap for catheterization of the UA. The DSA-like images were scored by the interventional radiologists in a binary manner as either "useful" or "not useful" for roadmapping.

Those that were graded "useful" were then validated against the original 3DRA scans to determine true positives and false positives due to foreshortening or vessel overlapping. The interobserver agreement on the scoring of these DSA-like images was calculated and is reported in Cohen's kappa statistics. The kappa coefficient gives a quantitative measure of the magnitude of agreement between observers.

Additionally, we quantified the distribution of anatomic variation in UA origin to confirm that this study included a broad distribution of patients, using the classification system established by Gomez-Jorge et al. (19).

Results

All 3DRAs acquired for the study were rated by both interventional radiologists to be of sufficient quality for identification of the UA origin and therefore useful as a roadmap. All 3DRA scans were of sufficient diagnostic quality for further analysis. The 3DRA image quality was graded good or excellent in 90.3% of the cases and fair in 9.7%. None of the cases was graded poor. There was no difference in grading between selective or aortic injection.

The angulations and rotations of the C-arm used during 3D roadmapping are plotted in Fig. 1. For both the left and right UA, two clusters are observed. Both clusters show a wide spread in projection angles between RAO 20° and 50°, and between LAO 20° and 50°. The caudal-cranial range was smaller with angulations, between Cran10 and Caud10.

The DSA-like images that were constructed from the 3DRA volumes were rated to be of sufficient quality for identification of the UA. The assessment of the DSA-like roadmap images was validated against the original 3DRA scans to determine true positives and false positives due to foreshortening or vessel overlapping (Fig. 2). The percentages of true and false positives for the six considered viewing angles are depicted in Fig. 3. More than 50% of the DSA-like images at RAO 45° and LAO 45° appeared to be adequate for UA catheterization. However, when validated against the 3DRA, false positives were identified due to unappreciated overlapping vessels. The number of false positives with respect to the total number of positive images indicates that, on average, in 28% of the cases the physician would be relying on an incorrect angle (Table 1). A fair overall interob-

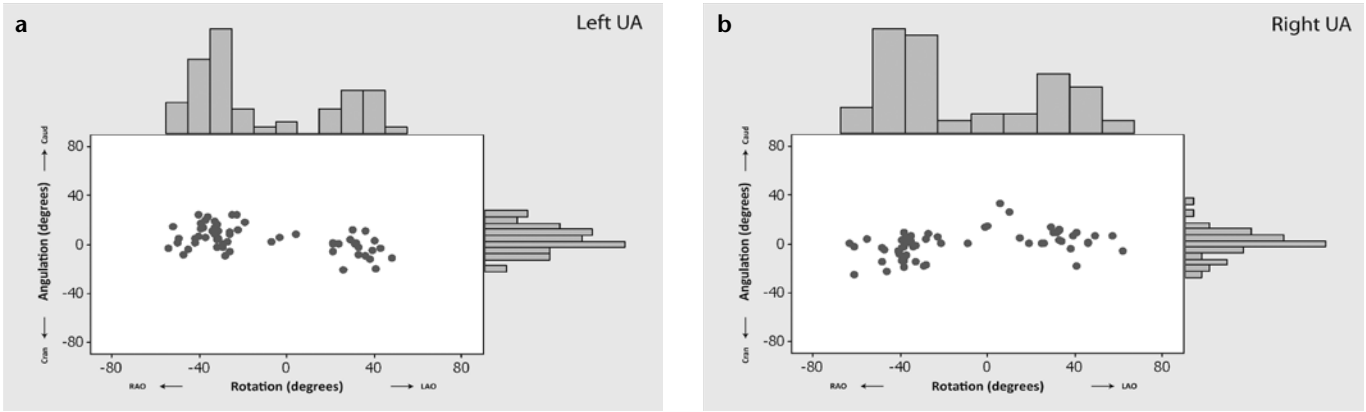

Figure 1. a, b. Scatter plots representing the spread of C-arm viewing angles selected for 3D roadmapping for the left **(a)** and right **(b)** uterine arteries. Caud, caudal; Cran, cranial; LAO, left anterior oblique; RAO, right anterior oblique; UA, uterine artery.

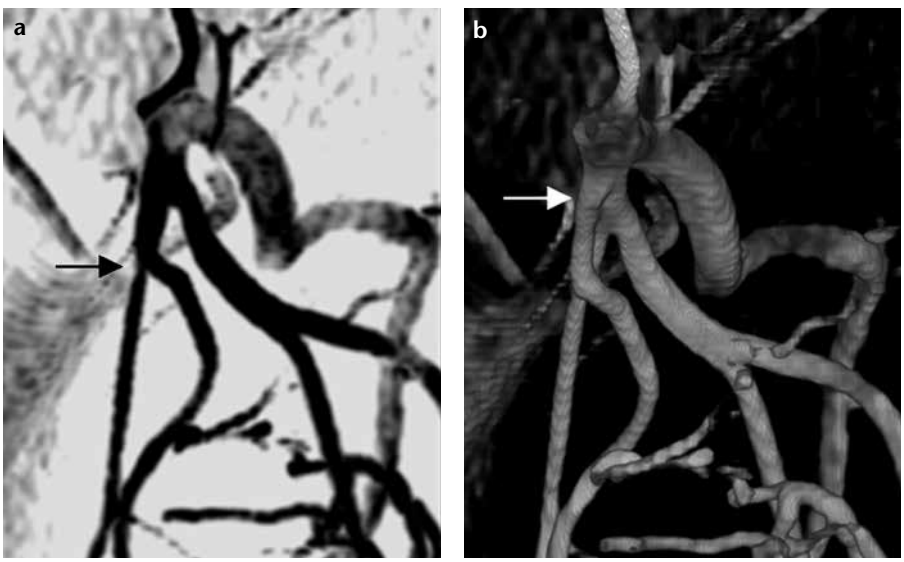

Figure 2. a, b. Comparison between a false positive 2D DSA-like image **(a)** and its corresponding 3D rotational angiography rendering **(b)**. On the 2D DSA image, the origin of the uterine artery deceptively appeared medially and distally *(***a,** *black arrow)*, while the 3D rotational angiography image definitively demonstrates that it arises anteriorly and proximally *(***b,** *white arrow)*.

server agreement on the scoring of the DSA-like images was found with a kappa value of 0.376 (range, 0.18–0.54).

The classification of all reviewed UAs into the distinct anatomic subtypes is given in Table 2. The most common branching for both the left and right UA is Type I, where the UA is the first branch of the inferior gluteal artery.

Discussion

This study investigated the benefits of using 3DRA over the use of standard angiographic projection angles for visualization of the origin of the UA in UAE procedures. Additionally, it assessed the variation in anatomy of the UA.

The set of viewing angles selected from a 3DRA for subsequent roadmapping reveal two clusters of preferred angles, however each with a wide spread (Fig. 1). This indicates that there are no standard preferred projection angles, but instead that multiple projection angles might suffice as roadmap. These results corroborate the findings of previous smaller studies. Bucek et al. (17) analyzed the angulations used with 3D roadmap on eight patients with a wide spread from LAO 45° to RAO 90° for the right UA, and LAO 81° to RAO 78° for left UA. Naguib et al. (18) used MR angiography to predict the best projection angle to visualize the origin of the UA in 20 patients. The best projection angles of the origin of the left UA varied between LAO 45° and RAO 45°, and the angulations for the right UA were determined to be between LAO 50° and RAO 50°.

Relying on a "standard" projection of LAO 45° or RAO 45° appears to clearly identify the UA origin on a 2D roadmap over 50% of the time, but actually is inadequate (often due to nonperceived overlapping vessels) more than 20% of the time (Fig. 3). The danger of using a false positive angle, where the origin of the UA is not located as expected from the DSA image, is that the interventionist could potentially spend a significant amount of time searching for the origin of the UA in an incorrect location (Fig. 2). This would result in added procedure time, elevated radiation dose, and potentially increased iodinated contrast usage.

The 3DRA volume allows the operator to select the optimal viewing angle to catheterize the UA, which might circumvent the need for multiple DSA runs to find the origin of the UA. It may therefore be expected that the use of 3DRA can contribute to lowering radiation exposure and contrast injections. Patient studies in neuroradiology have shown that the use of 3DRA for 3D roadmapping and pretreatment selection of optimal working projections can lead to radiation dose reduction for cases requiring multiple oblique 2D DSA runs (20–22). Similarly, a recent multicenter comparison has shown that the use of 3DRA for carotid artery treatment involves a cumulative radiation dose three times lower than that for procedures based on 2D angiography only, mainly due to quicker selection of working projections and consequent reduction in fluoroscopy time and number of 2D DSA series (23).

The interobserver agreement of the

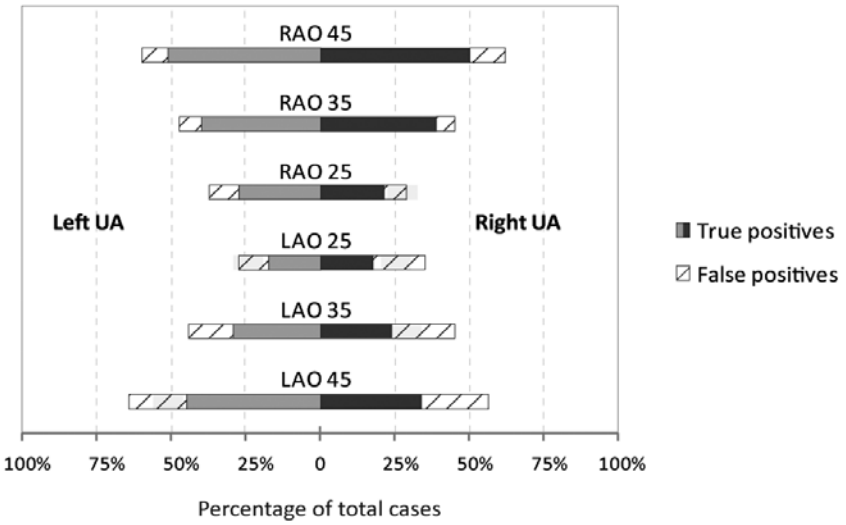

Figure 3. Percentage of cases in which the angiographic viewing angles were scored useful (positive) for roadmapping to catheterize the left and right uterine artery. The positively scored cases are divided into true and false positives. More than 50% of the 2D roadmap-like images at right anterior oblique angle of 45° and left anterior oblique angle of 45° appeared to be adequate for uterine artery catheterization. However, when validated against the 3D rotational angiography, false positives were identified due to unappreciated overlapping vessels.
LAO, left anterior oblique; RAO, right anterior oblique; UA, uterine artery.

Table 1. Percentage of cases in which the angiographic viewing angles were scored useful (i.e., positive) for roadmapping to catheterize the left and right uterine artery; divided into true positives and false positives

	Left UA	Right UA	Total
TP angles	35.1%	31.1%	33.1%
FP angles	11.6%	14.5%	13.0%
Total positive angles (TP+FP)	46.7%	45.6%	46.1%
Deceptive angles (FP/Total positives)	24.8%	31.8%	28.2%

The percentages given are averages of the six considered viewing angles for each UA. From the false positives, the percentage of deceptive angles was calculated. On average in 28% of the cases physicians would rely on the wrong roadmap.
FP, false positive; TP, true positive; UA, uterine artery.

Table 2. Anatomical classification of 122 uterine arteries reviewed

UA classification[a]	Left UA (n=61)	Right UA (n=61)	Total (n=122)
Type I	67.2%	55.7%	61.5%
Type II	19.7%	16.4%	18.0%
Type III	4.9%	23.0%	13.9%
Type IV	6.6%	4.9%	5.7%
Unclassifiable	1.6%	0.0%	0.8%

[a]Type I, the uterine artery as first branch of the inferior gluteal artery; Type II, the uterine artery as second or third branch of the inferior gluteal artery; Type III, the uterine artery, the inferior gluteal and the superior gluteal arteries arising as a trifurcation; Type IV, the uterine artery as first branch of the hypogastric artery (22).
UA, uterine artery.

usefulness of DSA-like images for roadmapping showed a fair average kappa value, which indicates that even two experienced interventional radiologists judge the usefulness of 2D images for roadmapping for UAE differently. It demonstrates the potential of 3DRA as a valuable tool to ensure an optimal visualization of the origin of the UA for all interventionists. Furthermore, interventionists with less experience in performing the treatment will always be able to find a suitable viewing angle with 3DRA, therefore also reducing the total amount of dose (13).

The anatomy of the UA can be categorized by the location of the origin of the artery. Our study showed a trend similar to the study from Kanasaki et al. (24), with Type I as the most common (62.1%) anatomical variant. Pelage et al. (25) looked into the division of the internal iliac artery, and their results corroborate our findings, with Type I and Type II origins noted in 77% of their cases, and 79% in ours. Interestingly, while in our study trifurcation origins (Type III) were noted in 14% of the patients, Gomez-Jorge et al. (19) reported 43% Type III. Their study identified the UA with the use of 2D images, which might have given a false indication of the origin of the UA due to vessel overlap, potentially resulting in a higher number of Type III classifications.

This study carries some limitations. First, the DSA-like images are not dynamic images like real DSA runs, in which vessel overlap might be better observed compared to static images. On the other hand, modern angiographic systems typically also use nondynamic imaging to create a 2D roadmap by stacking all the images obtained during the roadmap acquisition. If one did have the advantage of being able to view a dynamic image during the roadmap run, this could potentially give a lower percentage of false positive roadmaps.

In addition, the choice of the six studied viewing angles might be a limitation, as different angles, including cranio-caudal angulation, might be used by some physicians as a first choice when performing UA catheterization. The direction (medial, lateral, or anterior) that the UA originates might influence the optimal position of the C-arm to visualize the origin of the UA. Worthington-Kirsch (26) examined the origin of the UAs for 25 consecutive cases and the findings showed that there is no standard direction that the UA branches off from the internal iliac artery. Angulation of the C-arm in cranial-caudal direction may therefore be advantageous to find

a good view to visualize the origin of the UA.

In this study, we focused on the variation in rotation of the C-arm for a good view on the origin of the UA. Our results suggest that 3DRA carries advantages over acquiring 2D DSA acquisitions from multiple viewing angles to find the origin of the UA, thereby potentially reducing radiation exposure. However, an extensive study with comparison of the dose and contrast for 2D and 3D roadmapping for UAE is required to further investigate this potential. In addition to 3DRA, MR angiography also provides insight into the complex pelvic vascular anatomy. With modern image fusion techniques, an MR angiography volume superimposed upon live fluoroscopy can be used for roadmapping during the interventional procedure, which may lead to even lower radiation dose and contrast usage. Navigation during UAE, facilitated by MR angiography roadmapping, is the subject of a future study.

In conclusion, our study shows that there are no standard projection angles to visualize the origin of the UA. Our results indicate that 3DRA is a valuable alternative to multiple 2D acquisitions and could reduce total patient radiation dose and contrast load. It can give the physician better insight into the origin of the UA, which is instrumental in prompt catheterization during UAE.

Conflict of interest disclosure

The authors declared no conflicts of interest.

References

1. Edwards RD, Moss JG, Lumsden MA, et al. Uterine-artery embolization versus surgery for symptomatic uterine fibroids. N Engl J Med 2007; 356:360–370. [CrossRef]
2. Hehenkamp WJ, Volkers NA, Birnie E, Reekers JA, Ankum WM. Symptomatic uterine fibroids: treatment with uterine artery embolization or hysterectomy--results from the randomized clinical Embolisation versus Hysterectomy (EMMY) Trial. Radiology 2008; 246:823–832. [CrossRef]
3. Maleux G, Timmerman D, Heye S, Wilms G. Acquired uterine vascular malformations: radiological and clinical outcome after transcatheter embolotherapy. Eur Radiol 2006; 16:299–306. [CrossRef]
4. Gupta JK, Sinha AS, Lumsden MA, Hickey M. Uterine artery embolization for symptomatic uterine fibroids. Cochrane Database Syst Rev 2006:CD005073.
5. Narayan A, Lee AS, Kuo GP, Powe N, Kim HS. Uterine artery embolization versus abdominal myomectomy: a long-term clinical outcome comparison. J Vasc Interv Radiol 2010; 21:1011–1017. [CrossRef]
6. Tropeano G, Amoroso S, Scambia G. Non-surgical management of uterine fibroids. Hum Reprod Update 2008; 14:259–274. [CrossRef]
7. Hirst A, Dutton S, Wu O, et al. A multi-centre retrospective cohort study comparing the efficacy, safety and cost-effectiveness of hysterectomy and uterine artery embolisation for the treatment of symptomatic uterine fibroids. The HOPEFUL study. Health Technol Assess 2008; 12:1–248.
8. Stokes LS, Wallace MJ, Godwin RB, Kundu S, Cardella JF. Quality improvement guidelines for uterine artery embolization for symptomatic leiomyomas. J Vasc Interv Radiol 2010; 21:1153–1163. [CrossRef]
9. Spies JB, Roth AR, Gonsalves SM, Murphy-Skrzyniarz KM. Ovarian function after uterine artery embolization for leiomyomata: assessment with use of serum follicle stimulating hormone assay. J Vasc Interv Radiol 2001; 12:437–442. [CrossRef]
10. Bratby MJ, Ramachandran N, Sheppard N, Kyriou J, Munneke GM, Belli AM. Prospective study of elective bilateral versus unilateral femoral arterial puncture for uterine artery embolization. Cardiovasc Intervent Radiol 2007; 30:1139–1143. [CrossRef]
11. Costantino M, Lee J, McCullough M, Nsrouli-Maktabi H, Spies JB. Bilateral versus unilateral femoral access for uterine artery embolization: results of a randomized comparative trial. J Vasc Interv Radiol 2010; 21:829–835. [CrossRef]
12. Sapoval M, Pellerin O, Rehel JL, et al. Uterine artery embolization for leiomyomata: optimization of the radiation dose to the patient using a flat-panel detector angiographic suite. Cardiovasc Intervent Radiol 2010; 33:949–954. [CrossRef]
13. Andrews RT, Brown PH. Uterine arterial embolization: factors influencing patient radiation exposure. Radiology 2000; 217:713–722.
14. Mori K, Saida T, Shibuya Y, et al. Assessment of uterine and ovarian arteries before uterine artery embolization: advantages conferred by unenhanced MR angiography. Radiology 2010; 255:467–475. [CrossRef]
15. Naguib NN, Nour-Eldin NE, Hammerstingl RM, et al. Three-dimensional reconstructed contrast-enhanced MR angiography for internal iliac artery branch visualization before uterine artery embolization. J Vasc Interv Radiol 2008; 19:1569–1575. [CrossRef]
16. Chun-Lin C, Hong-Xia G, Ping L, et al. Three-dimensional reconstruction of the uterine vascular supply through vascular casting and thin slice computed tomography scanning. Minim Invasive Ther Allied Technol 2009; 18:98–102. [CrossRef]
17. Bucek RA, Reiter M, Dirisamer A, Kettenbach J, Lammer J. Three-dimensional digital rotation angiography for embolization therapy of uterine leiomyomas: first results. Rofo 2004; 176:1001–1004. [CrossRef]
18. Naguib NN, Nour-Eldin NE, Lehnert T, et al. Uterine artery embolization: optimization with preprocedural prediction of the best tube angle obliquity by using 3D-reconstructed contrast-enhanced MR angiography. Radiology 2009; 251:788–795. [CrossRef]
19. Gomez-Jorge J, Keyoung A, Levy EB, Spies JB. Uterine artery anatomy relevant to uterine leiomyomata embolization. Cardiovasc Intervent Radiol 2003; 26:522–527. [CrossRef]
20. Schueler BA, Kallmes DF, Cloft HJ. 3D cerebral angiography: radiation dose comparison with digital subtraction angiography. AJNR Am J Neuroradiol 2005; 26:1898–1901.
21. Wong SC, Nawawi O, Ramli N, Abd Kadir KA. Benefits of 3D rotational DSA compared with 2D DSA in the evaluation of intracranial aneurysm. Acad Radiol 2012; 19:701–707. [CrossRef]
22. Gupta A, Radaelli AG. Live 3D guidance in endovascular procedures. Endovascular Today 2009; July:28–40.
23. Tsapaki V, Vano E, Muavrikou I, et al. Comparison of patient dose in two-dimensional carotid arteriography and three-dimensional rotational angiography. Cardiovasc Intervent Radiol 2008; 31:477–482. [CrossRef]
24. Kanasaki S, Furukawa A, Wakamiya M, et al. The vascular anatomy of the female pelvis artery and optimal projection angle to evaluate a uterine artery furcation: investigation with 3D-CT. Paper presented at: CIRSE 2010; October 2-6, 2010; Valencia, Spain.
25. Pelage JP, Le Dref O, Soyer P, et al. Arterial anatomy of the female genital tract: variations and relevance to transcatheter embolization of the uterus. AJR Am J Roentgenol 1999; 172:989–994. [CrossRef]
26. Worthington-Kirsch RL. Anatomy of the uterine artery. AJR Am J Roentgenol 2000; 174:258. [CrossRef]